Star and linear dunes on Mars

Kenneth S. Edgett and Dan G. Blumberg

Department of Geology, Arizona State University, Box 871404, Tempe, Arizona 85287-1404, USA

Abstract. A field containing 11 star and incipient star dunes occurs on Mars at 8.8°S, 270.9°W. Examples of linear dunes are found in a crater at 59.4°S, 343°W. While rare, dune varieties that form in bi- and multidirectional wind regimes are not absent from the surface of Mars. The occurrence of both of these dune fields offers new insight into the nature of martian wind conditions and sand supply, The linear dunes appear to have formed through modification of a formerly transverse aeolian deposit, suggesting a relatively recent change in local wind direction. The 11 dunes in the star dune locality show a progressive change from barchan to star form as each successive dune has traveled up into a valley, into a more complex wind regime. The star dunes corroborate the model of N. Lancaster (1989, *Progress in Physical Geography 13*, 67–91; 1989, *Sedimentology 36*, 27–289) for the formation of star dunes by projection of transverse dunes into a complex, topographically influenced wind regime. The star dunes have dark streaks emanating from them, providing evidence that the dunes were active at or near the time the relevant image was obtained by the Viking 1 orbiter in 1978. The star and linear dunes described here are located in different regions on the martian surface. Unlike most star and linear dunes on Earth, both martian examples are isolated occurrences; neither is part of a major sand sea. Previously published Mars general circulation model results suggest that the region in which the linear done field occurs should be a bimodal wind regime, while the region in which the star dunes occur should be unimodal. The star dunes are probably the result of localized complication of the wind regime owing to topographic confinement of the dunes. Local topographic influence on wind regime is also evident in the linear dune field, as there are transverse dunes in close proximity to the linear dunes, and their occurrence is best explained by funneling of wind through a topographic gap in the upwind crater wall.

received 13 December 1993, revised 7 July 1994, published December 1994

Citation: Edgett, K. S. and D. G. Blumberg (1994) Star and linear dunes on Mars, *Icarus 112*(2), 448–464, doi:10.1006/icar.1994.1197.

Introduction

Aeolian dunes with morphologies that form in multi-directional wind regimes are rare on Mars (Greeley et al. 1992). The fact that such dunes appear to be lacking is particularly striking because more than half of Earth's desert aeolian dunes are classified as linear and star dunes; forms that occur in bi- and multi-directional wind conditions, respectively (Fryberger 1979, Lancaster 1982, 1989a, 1989b, Tsoar 1989). The occurrence of linear or star dunes has important implications for interpretation of both wind regime and sand supply (Wasson and Hyde 1983).

Most aeolian dunes seen in Mariner 9 and Viking 1 and 2 orbiter images were identified as barchan, barchanoid, transverse, or complex dunes that combine aspects of these dune type (Cutts and Smith 1973, Breed 1977, Breed et al. 1979b, Tsoar et al. 1979, Thomas 1984, Greeley et al. 1992). These dune types result from winds that foster sand transport from one dominant direction (Bagnold 1941, McKee 1978, Pye and Tsoar 1990). A good example of the effects of unidirectional wind is an intracrater dune field located in Oxia (Western Arabia) at 1.9°N, 351.7°W (Figure 1) which has dark barchan dunes with horns that point in the same direction (downward) as a dark streak that emanates from the crater (see Viking image 655A69).

This article presents two unambiguous examples of martian dunes that formed in bi- and multi-directional wind regimes. The first is a field of 11 dunes, located at 8.8°S, 270.9°W, with star and incipient star morphologies indicative of a multidirectional wind regime (Figure 2). The second is a dune field in the southern middle latitudes (59.4°S, 343°W) which contains linear dunes resulting from bidirectional wind conditions (Figure 3). Six additional dune fields containing possible star or linear duns are briefly described.

Previous Identifications

Some dunes in the martian north polar sand sea have minor, superposed ridges indicating weaker secondary wind directions (Tsoar et al. 1979, Breed et al. 1979b). Tsoar et al. (1979) noted that there are incipient linear dunes formed by elongation of barchan horns in the north polar erg, but there are no martian sand seas which consist almost entirely of linear dunes similar to those in Africa and Australia (Wasson et al. 1988, Lancaster 1989c). Lee et al. (1993) found additional dunes in the north polar sand sea which appear to have formed by elongation of barchan horns. The north polar erg linear dunes are the subject of a recent article by Lee and Thomas (1994) and are not discussed further here except to note that they appear to be an isolated occurrence related to local wind influenced by topographic features, as may be the case for the dunes that we describe in this article (Figures 2 and 3).

Figure 1. Small, dark, barchan dunes on a crater floor in Oxia. These dunes are moving toward the southwest (lower left), the same direction as dark wind streaks emanating from similar intracrater dunes in the region. Illumination is from the left. Viking image 709A42, centered at 1.9°N, 351.7°W.

Sinuous ridges that have been partly exhumed from beneath a thick, mantling deposit in Dorsa Argentea (77°S, 30°W) have also been proposed to be linear dunes (Ruff 1992). The Dorsa Argentea ridges have been interpreted as the result of a variety of possible processes, including aeolian, glacial, volcanic, and fluvial events (Ruff and Greeley 1990, Kargel and Strom 1992, Rice and Mollard 1994). Ruff (1992) presented evidence that the Dorsa Argentea ridges have many morphologic similarities to terrestrial stabilized linear dunes, but interpretation of the ridges' origins remains problematic (Ruff 1994).

Prior to the present study, one dune field located at 57.5°S, 19.8°W in Darwin Crater was suggested by Breed et al. (1982, Fig. 17b) to be a possible star dunes (see Figure 4). Other southern hemisphere intracrater dune fields have complex transverse forms and large echo dunes formed by interaction of wind with crater wall topography (Cutts and Smith 1973, Lancaster and Greeley 1987).

The Martian Star Dune Example

Background

Lancaster (1989a) reviewed terrestrial star dune morphologies and occurrences. Star dunes cover about 5% of terrestrial dune areas. Star dunes typically have a pyramid shape with multiple slip (avalanche) faces and three or four arms radiating from a central peak. The arms on a star dune are usually not equally developed; many star dunes have developed dominant or primary arms oriented in a preferred direction related to the strongest winds that affect the region. Breed and Grow (1979) classified star dunes as simple (three or four arms, slip faces about the same size), compound (large primary arms with small subsidiary arms), and complex (large dunes with combined characteristics of star and other dune types).

Star dunes generally form from a relatively large volume of sand that has been trapped by the combined influences of topography and seasonal variations in wind speed and direction (Lancaster 1989a, b). Lancaster (1989a) concluded that most published observations of star dune morphology and occurrence suggest that they form by modification of preexisting dunes as they migrate or extend into an area of opposing or multidirectional wind conditions. Based on observations of dunes in the Gran Desierto, Mexico, Lancaster (1989a, b) proposed a model in which a transverse dune moves into an area subjected to a seasonal reversal of wind directionality. This "reversing dune" begins to develop a third arm perpendicular to the main wind direction as secondary winds in the lee of the dune develop and cause an inflow of air (and sand) around the center of the dune ridge. The development of third and fourth arms is reinforced by the dune shape and by migration into multidirectional winds. The winds from different directions are typically not equal in strength, and their direction is usually related to seasonal changes. Nielson and Kocurek (1987) found that small star dunes near Dumont, California, could break up into barchans and then re-form as star dunes as a function of seasonal changes in wind direction and complexity, perhaps indicating that there is a minimum survival size or sand supply required to make permanent star dunes. Blount (1988, p. 137) observed that large star dunes in the Gran Desierto tend to have pitted surfaces at their interdune margins, suggesting that in some cases the star dune morphology is self-reinforcing and actually contributes to local erosion and deposition of sand on the star dune.

Observations and Interpretations

The star dunes at 8.8°S, 270.9°W are shown in Figure 2. Located in the classic low-albedo region Mare Tyrrhenum, the dunes are dark relative to their surroundings (the term, classic, here refers to the pre-spacecraft nomenclature for regional albedo features;

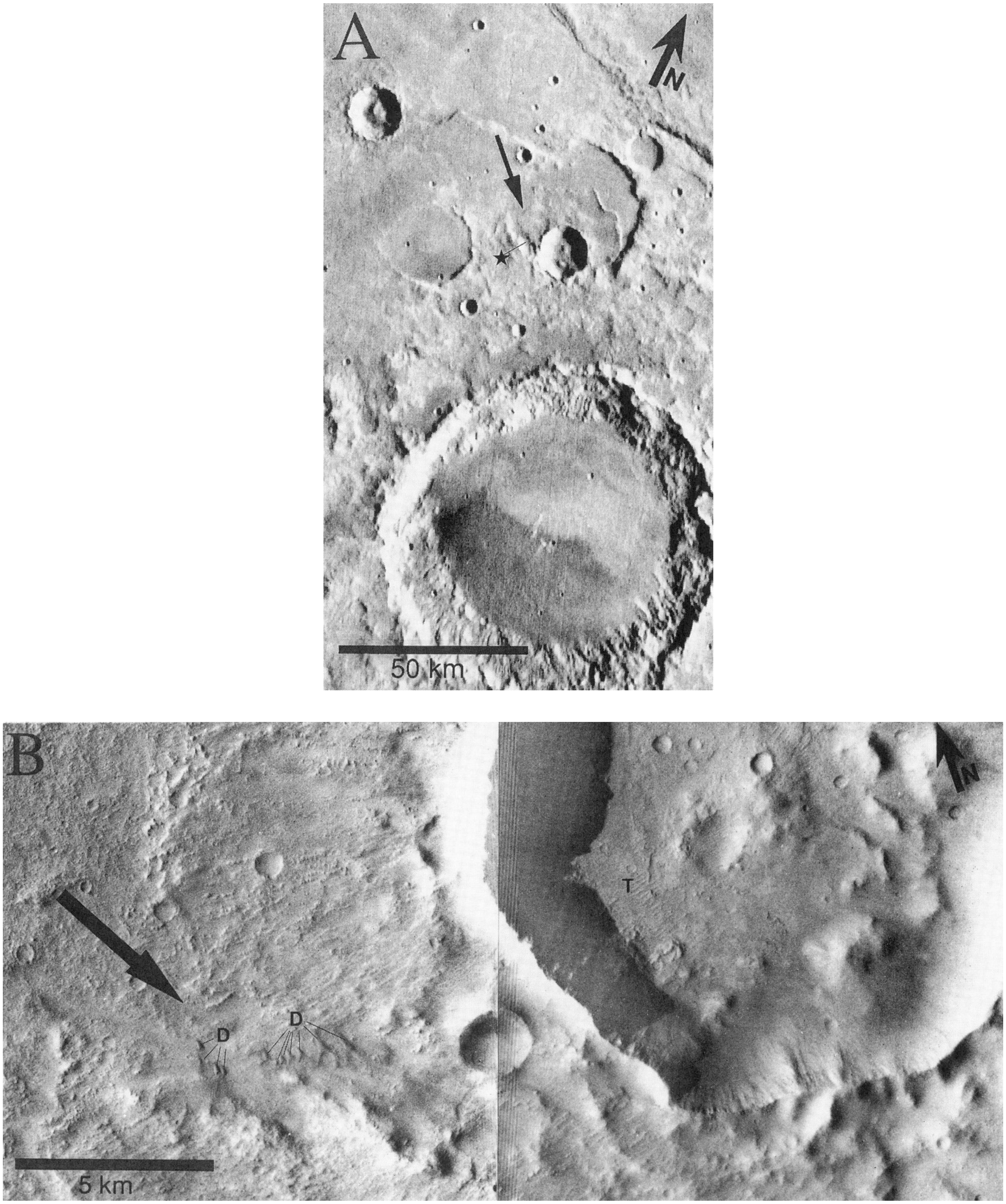

Figure 2. Martian star dunes located at 8.8°S, 270.9°W. **(A)** Regional setting. The dunes are nestled in a valley formed by the junction of rater rims (star). The dominant regional winds blow toward the south–southeast (arrow). Briault Crater is at the bottom of the frame; illumination is from the right. Viking image 378X11. **(B)** The star dunes (D). Dominant regional winds are indicated by the arrow. Note small transverse dune forms (T) on the crater floor east of the star dunes. Illumination is from the left. Mosaic of Viking images 755A19 and 755A21, obtained in 1978 when Mars was at L_s 113°, southern winter. **(C)** see next page.

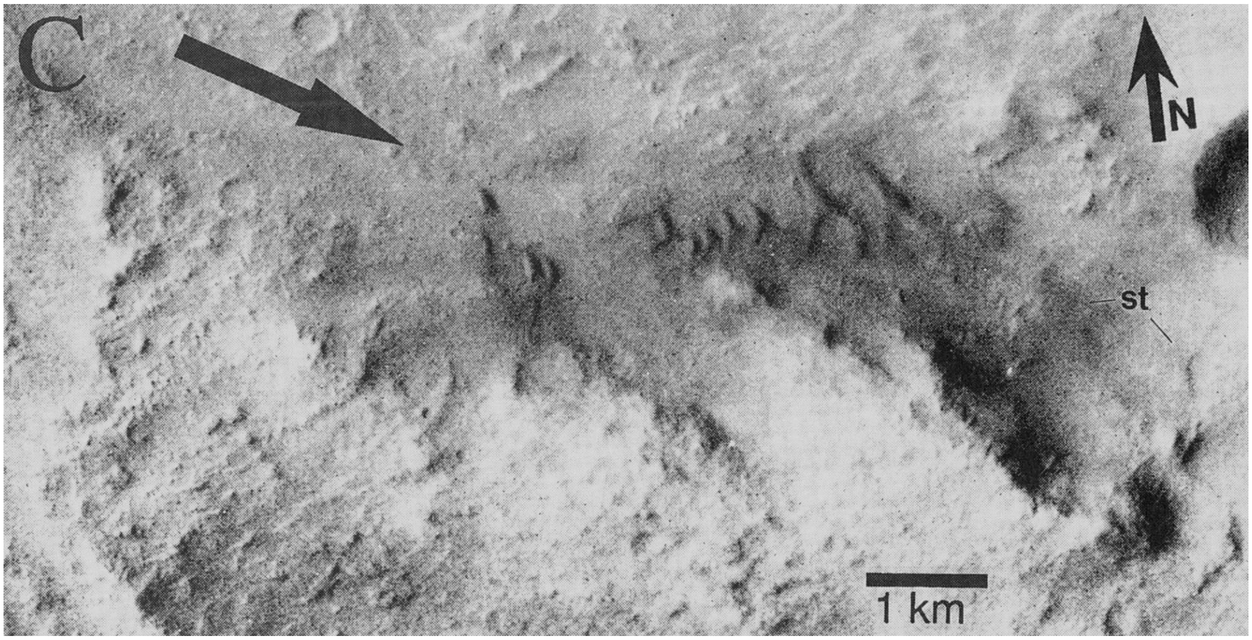

Figure 2, continued. (C) Magnified view of the star dunes. Note dark streaks emanating from the dunes (st), probably indicating deflation of sand at or near the time the image was obtained. Part of Viking image 755A19.

see Antoniadi 1930). They occur in a valley created by the junction of two crater rims (Figure 2a); one crater is smaller (15 km diameter) and superposed on the rim of the other (45 km diameter) The valley is located about 30 km northwest of Briault Crater (10°S, 270°W), a 90-km-diameter impact feature that contains a dark, presumably sandy aeolian deposit (cf. Thomas 1984, Edgett and Christensen 1994).

In Figure 2 there are 11 distinct dunes showing different states of radial arm development. Indeed, there is a progression from barchan morphologies in the west to three-armed stars in the east. Two of these dunes (second and third from the last at the eastern end of the valley) have particularly well-developed arms. The larger star dune is about 1 km wide at its greatest extent. Some of the dunes at the east end of the valley have dark, wispy streaks emanating from them ("st" in Figure 2c).

Discussion

The dark streaks coming from the dunes (Figure 2c) are oriented toward the south-southeast, and some can be traced up to 3 km beyond the dunes. We propose that these streaks indicate the direction of the most recent sand-moving events which occurred prior to the acquisition of the Viking image. Furthermore, we propose that the presence of these dark streaks indicates that the dunes in Figure 2 were active as recently as 1978. The image in Figures 2b and 2c was obtained when Mars was at L_s 113° (southern winter). Prior to that time, Mars was under global dust storm conditions twice in 1977, between L_s 180° and 340° in southern spring/summer (Kahn et al. 1992, Table III). If we assume that global dust storm sediments (approximately ≤ 10-μm particles) settle out of the atmosphere in a nearly uniform, optically thick, light-hued coating, then we can conclude that dark surfaces occur where the bright dust coating has been removed. The presence of dark, wispy streaks in Figure 2c is then consistent with the burial or removal of bright dust on the non-dune surfaces to the south–southeast of the star dunes. The streaks must have formed during a period of less than 6 months between the end of the second global dust storm in 1977 and the time when the image was obtained in mid-1978. If a northwesterly wind blew sand from the star dunes to create the streaks, then the dunes also must be considered active.

The dominant wind in the vicinity of the star dunes in Figure 2 is unidirectional and blows from the north–northwest, as indicated by the dark streaks ("st" in Figure 2c) and transverse dunes inside the 15-km-diameter crater east of the dune field (T in Figure 2b). That this is the dominant wind direction is corroborated by (1) regional geomorphic evidence and (2) general circulation modeling. The pattern of dominant regional wind flow is indicated by the orientations of seasonally variable bright (dust) wind streaks, which match the position of dark intracrater (sand) deposits during southern summer (Arvidson 1974, Thomas 1982). Table 1 and Figure 5, derived from the Pollack et al. (1990) general circulation model (GCM) results presented by Skypeck (1989) and Greeley et al. (1993), also shows that the strongest winds in the vicinity of the star dune field should occur in southern summer (see L_s 284° in Figure 5 and Table 1), and that wind magnitude and direction both shift somewhat as a function of season.

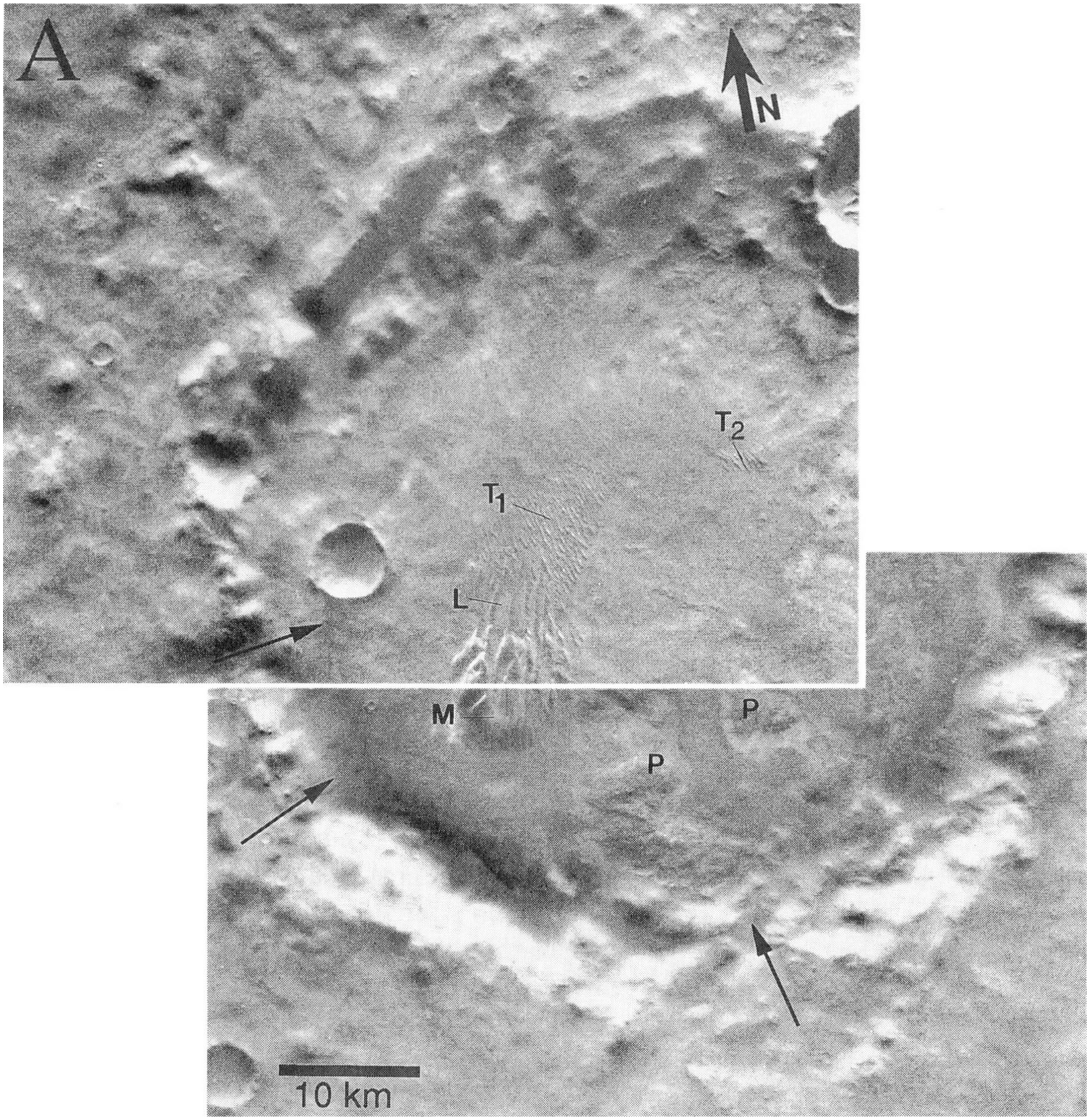

Figure 3. Martian linear dunes in a crater located at 59.4°S, 343°W. **(A)** Linear dune forms are indicated by L. Linear dunes emanate from the barchanoid dune mass, M. Further downwind, the linear dunes grade into transverse dunes (T_1). Another field of transverse dunes occurs about 8 km downwind of the main dune field, at the break in slope between the crater wall and floor (T_2). Pits, possibly formed by aeolian deflation, are found at P. Interpreted wind flows are indicated by thin arrows. Illumination is from the top. This is a mosaic of Viking images 573B30 and 573B32, obtained in 1978 at L_s 59.6°, southern autumn. **(B)** See next page.

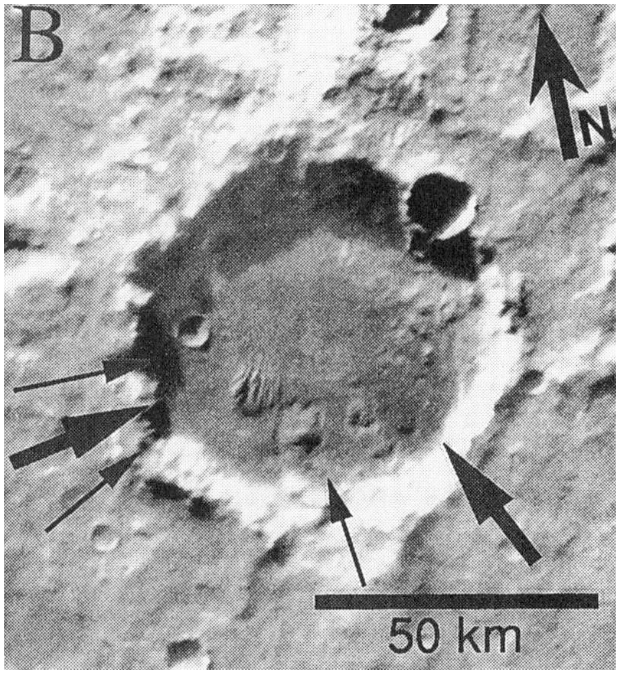

Figure 3, continued. (B) Lower-resolution view, showing more clearly the topographic variations along the crater rim that might have contributed to the morphological expression of the dunes by channelizing wind. Dominant regional winds (from general circulation model; Greeley et al. 1993) are indicated by heavy arrows; interpreted channelized winds are shown by thin arrows (arrow length has no particular significance). Viking image 358S03, illuminated from the top.

The star dunes, which require multidirectional winds, occur in a region that has unimodal winds because of their local topographic confinement. The gap between the superposed crater rims (Figure 2a) opens out toward the north–northwest, and the dominant winds are north–northwesterly; thus the valley has acted as a funnel by bringing into it both the dominant regional wind and the sand that has been picked up along the way. The topography of the valley walls likely provides the necessary multidirectional winds needed for star dune development. Examples of star dunes forming in narrow valleys with surrounding high topography are found in North American deserts, particularly the Basin and Range region (Smith 1982, Nielson and Kocurek 1987, Blumberg and Greeley 1993).

Star dunes in Death Valley, California, are illustrated in Figure 6. Unlike the dunes in Figure 6, the martian star dunes in Figure 2 are very simple and resemble the "textbook case" of three-armed star dune development rather than the complex star dune types more commonly seen on Earth (Thomas 1989, Lancaster 1989a). We found only one literature reference showing a photograph of simple three-armed star dunes (Breed and Grow 1979, Fig. 179a); even this particular example, located in the Mexican Gran Desierto, does not resemble very closely the martian dunes in Figure 2. Sometimes the shape of a large, topographically trapped dune near Bruneau, Idaho (Greeley et al. 1971, 1974, Murphy and Greeley 1972), is organized in a star-like form that is similar to the star dunes at the eastern end of the valley in Figure 2 (Smith 1982, Fig. 11-21). However, the shape of the Bruneau dune varies from year to year (Murphy 1975).

Figure 4. Possible complex star dune (arrow) located in a pit on the floor of Darwin Crater at 57.5°S, 19.8°W. This dune was identified by Breed et al. (1982) as a possible star dune. This is a part of Viking image 533B50; illumination is from the top.

The simplicity of the star dunes in Figure 2 suggests that the winds that have influenced these dunes are multidirectional but do not have a very complex pattern of variation. The dunes show a progression from barchan shapes at the western end of the valley to tri-armed stars at the eastern end. Barchan dunes tend to migrate laterally, whereas star dunes remain in one place. Thus, it would appear that as successive barchans migrated in the valley (Figure 2), they became trapped at the downwind (eastern) end and piled up to form star dunes. Winds coming off the valley slopes to the east and south (perhaps backflow from the otherwise northwesterly wind) probably created the slightly complex wind directionalities which led to the development of star dunes. Lancaster's (1989a) suggestion that star dunes form as other dune types migrate into areas with complex winds is corroborated by the nature of the 11 dunes in Figure 2.

There are no obvious sources for the sand that makes up the dunes shown in Figure 2. However, they occur in Mare Tyrrhenum, a classic low-albedo region. If we accept the premise that low-albedo regions have abundant dark, unconsolidated sand (e.g., Edgett and

Table 1. Wind direction and estimated surface shear stress from General Circulation model[a]

Season	L_s	shear stress[b] x 10^{-4} N m^{-2} (wind direction)[c] Linear dunes 59.4°S, 343°W (Figure 3)	Star dunes 8.8°S, 270.9° W (Figure 2)	Nili dunes 8.9°N, 292.8°W (Figure 11)	Run[d]	τ^e	Comments
S. autumn	46°	105 (NE)	15 (NW)	10 (NW)	87.42	0.3	
S. winter	106°	70 (NE)	15 (W)	25 (NE)	87.41	0.3	
S. winter	164°	60 (ENE)	5 (W)	20 (WNW)	87.40	0.3	
S. spring	218°	80 (NW)	15 (SE)	25 (SW)	87.39	2.5	developing dust storm phase
S. summer	284°	20 (NW)	75 (SSE)	70 (SW)	87.34	5.0	fully developed dust storm
S. summer	345°	5 (NW)	5 (SE)	10 (SE)	87.35	0.5	dust storm in decay

a Results estimated for three martian dune fields using the figures presented by Skypeck (1989), which were published by Greeley et al. (1993).

b Surface wind shear stress estimated by Skypeck (1989) from runs of the Pollack et al. (1990) general circulation model. These values are averaged over 7° x 9° latitude–longitude bins, and therefore should not be considered as measures of potential sand transport, but rather as indicators of the relative differences in magnitude from season to season. For comparison, the minimum shear stress needed to move 160 µm sand is about 550 x 10^{-4} N m^{-2}.

c Direction wind is flowing. For example, a southeasterly wind blows to the northwest, NW.

d Run numbers: see Greeley et al. (1993). Refers to the year (1987) and number of each Pollack GCM run.

e τ is atmospheric dust opacity, a parameter in the general circulation model.

Christensen 1994), then dunes located in topographic traps should be expected. However, the sand available for aeolian transport in this region is probably relatively scarce, as indicated by the fact that the dunes enter the valley as barchans and form distinct, individual dunes rather than a massive sand sea. Thus, despite the occurrence of star dunes, the region in which they occur has a unidirectional wind and a relatively low abundance of loose sand. The star dunes formed by the combined influence of topographic confinement and topographically induced polymodal winds acting on a volume of sand that is large relative to the area in which it is deposited.

The Martian Linear Dune Example

Background

Linear dunes constitute about half of all dune surfaces on Earth (Lancaster 1982). Linear dunes consist of three basic types—lee, seif, and vegetated—all of which advance by elongation downwind (Tsoar 1989). Seif and vegetated dunes that are presently active tend to occur in bidirectional wind regimes (Tsoar 1989, Thomas 1989). Seif and lee dunes have essentially similar morphologies, but lee dunes can occur in a unidirectional wind regime. Lee dunes form on the downwind side of obstacles such as a cliff, and occur where the brink of the cliff juts out and creates a convergence of wind streams (Tsoar 1989). Seif and lee dunes have sharp crests that run parallel to the resultant downwind direction. Seif dunes occur in bimodal wind regimes where the two wind directions meet the dune crest at oblique angles (Tsoar 1989, Thomas 1989). Typical examples of seif dunes are found in the Namib (Southwestern Africa), Rub' Al Khali (Arabia), and the Sinai Desert (Breed et al. 1979a, Tsoar 1983, 1989, Lancaster 1989c). In general, seif dunes arise by elongation of ridges and horns in barchan or transverse dunes moving into a bimodal wind regime, or from linear zibar (coarse-grained) dunes (Bagnold 1941, Lancaster 1982, Tsoar 1989). The origin of vegetated linear dunes is less well understood (Tsoar 1989); however, dunes with vegetation are unlikely to occur on Mars.

Observation and Interpretations

The most unambiguous examples of linear dunes found on Mars occur within a 70-km-diamter crater located at 59.4°S, 343°W (Figure 3). This crater is about 220 km southeast of Russell Crater, which contains a similarly large sand sea (1365 km^2; Peterfreund 1985). The linear dune area (Figure 3) is one of the southernmost dune fields of the Hellespontus region, a zone of thick intracrater sand accumulation (Cutts and Smith 1973, Breed 1977, Thomas 1984, Edgett and Christensen 1991). The entire dune field is about 25 km long, with a second smaller dune field occurring to the north–northeast after an ~8-km gap ("T_2" in Figure 3a). The linear dunes (L) occur in the middle of the main dune field. They are about 4 to 5 km long and originate in a barchanoid dune mass (M) 10 km wide by 8 km long. The linear dune ridges grade downwind into transverse dunes (T_1). The crater floor is pitted to the south–southeast of the dune field (Figure 3). The pits might be the result of aeolian deflation of crater floor materials which were subsequently reworked to form the dunes, as suggested by Thomas (1984) for other Hellespontus intracrater dune fields.

The linear dune ridges in Figure 3a are interpreted to be seif dunes based on similarity to two examples of seif-type dunes emanating from barchanoid dune masses found on Earth. The first, illustrated in Figure 7,

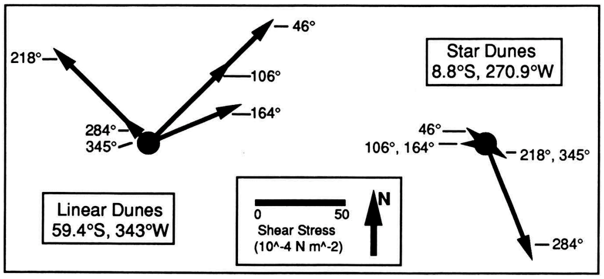

Figure 5. Modern wind direction and shear stress as a function of Ls (given next to each arrow) in the vicinity of the linear and star dunes as predicted by the general circulation model (GCM) maps of Skypeck (1989) and Greeley et al. (1993). According to the GCM predictions, the linear dune field occurs in a bimodal wind regime, wherein relatively strong winds blow toward the northeast in autumn and winter and less strong winds blow to the northwest during spring and summer. The star dune field is in a unimodal wind regime, with the strongest winds occurring in summer. These vectors are the same as listed in Table 1 and indicate direction and magnitude of wind for the 7° x 9° latitude–longitude bin in which each dune field occurs. Season (L_s) is given for each vector in degrees (see Table 1). The shear stresses are averaged for each latitude–longitude bin, and thus should not be considered as measures of potential sand transport, but rather as indicators of relative differences in wind magnitude as a function of season. For comparison to shear stresses presented here, the minimum shear stress needed to move 160 μm sand under average martian conditions is about 550 x 10^{-4} N m^{-2}.

occurs among the Shifting Sand Dunes of Christmas Lake Valley, Oregon, in the northern part of the North American Great Basin. The active dunes at the western end of this dune field are mostly barchanoid with superposed longitudinal ridge structures which give many of them the appearance of half a lima bean or pelecypod shell when observed from above (Allison 1966, Forbes 1973, p. 172). An example of this type of modified barchanoid dune is seen in the lower left corner of Figure 7, just above the scale bar. In some parts of the dune field, particularly upwind where sand is still being deflated from the basin floor, some of the barchanoid dunes have coalesced and the superposed longitudinal ridges have become extended in the downwind direction (center of Figure 7). Field investigation by author K. S. E. has shown that the linear ridges in Figure 7 have classic seif dune morphologies. The ridged texture on these dunes is though to be the result of season-dependent direction changes under bimodal wind conditions (Allison 1966). The winds currently acting on these dunes are characterized as "strong" and southwesterly in northern summer, changing 90° to northwesterly in winter (Berry 1963, p. 188). The northwesterly wind is not thought to be as strong or as persistent as the southwesterly wind; thus the overall wind conditions are consider to be "weakly" bimodal (Berry 1963, Allison 1966).

The second example is found in the Stovepipe Wells Dune Field (Figure 6), which covers approximately 100 km^2 in northern Death Valley, California. Four dune types, each characteristic of different wind conditions, are found at Stovepipe Wells: star, reverse transverse, barchans, and linear dunes (Smith 1982, Blumberg and Greeley 1993). The occurrence of so many dune types in close proximity is relatively rare and is attributed to local modification of winds by the influence of topography, as observed by author D. G. B. and discussed further below. The linear dunes at Stovepipe Wells ("L" in Figure 6) are similar to those in Christmas Lake Valley, Oregon (Figure 7), because they also emanate from features ("M" in Figure 6) resembling highly modified barchanoid dunes. Likewise, the martian dunes in Figure 3 (though approximately five times larger) are morphologically similar to the terrestrial examples in Figures 6 and 7.

Discussion

Linear seif dunes require bimodal winds in which to form (Tsoar 1989). However, the linear dunes in Figure 3a grade downwind into transverse dunes. As in the Stovepipe Wells dune field described above, this observation suggests that there might be local, rather than regional, controls on wind direction and dune morphology. The GCM results from Skypeck (1989) and Greeley et al. (1993) suggest that the autumn and winter winds are southeasterly (Figure 5, Table 1). Winds are strongest in autumn and spring. The linear dunes are extended toward the north–northeast, suggesting that the resultant wind is south–southwesterly. Such a direction is consistent with the GCM results that indicate a strong southwesterly wind in autumn and slightly weaker southeasterly winds in spring (Figure 5, Table 1). No other dune field in the Hellespontus region contains linear dunes. However, no other Hellespontus dune field occurs in an area (along 60°S) where the GCM predicts bimodal winds.

While the orientation of the linear dunes appears to be consistent with the regional winds predicted by the GCM, the orientation of transverse dunes north of the linear dunes is not. The transverse dune ridges ("T_1" in Figure 3a) are arranged perpendicular to the southwesterly wind flow. Some of the sand deflated from the main dune field has blown across an ~8-km gap to the northeast and piled up at the break in slope between crater floor and crater wall ("T_2" in Figure 3a).

The occurrence of the transverse dunes ("T_1" and "T_2" in Figure 3), which seem to defy the bimodal regional wind pattern, are probably the result of channelized winds. Winds channelized by topographic barriers and gaps can cause dune morphologies or orientations that are inconsistent with regional wind patterns (Tsoar and Blumberg 1992). An excellent example of local topographic effects on wind and dune patterns is found in the Stovepipe Wells dune field (Figure 6). Nearby wind measurements show that the predominant wind directions in the north part of Death Valley are from the northwest and southeast (Blumberg 1993, p. 33–58). However, the linear dunes are elongating to the east. Airmasses that flow down Emigrant Canyon, a topographic gap to the southwest of the dune field, provide the northwest wind component. Northwesterlies flowing through Death Valley are then diverted to become west–northwesterly to create a resultant sand

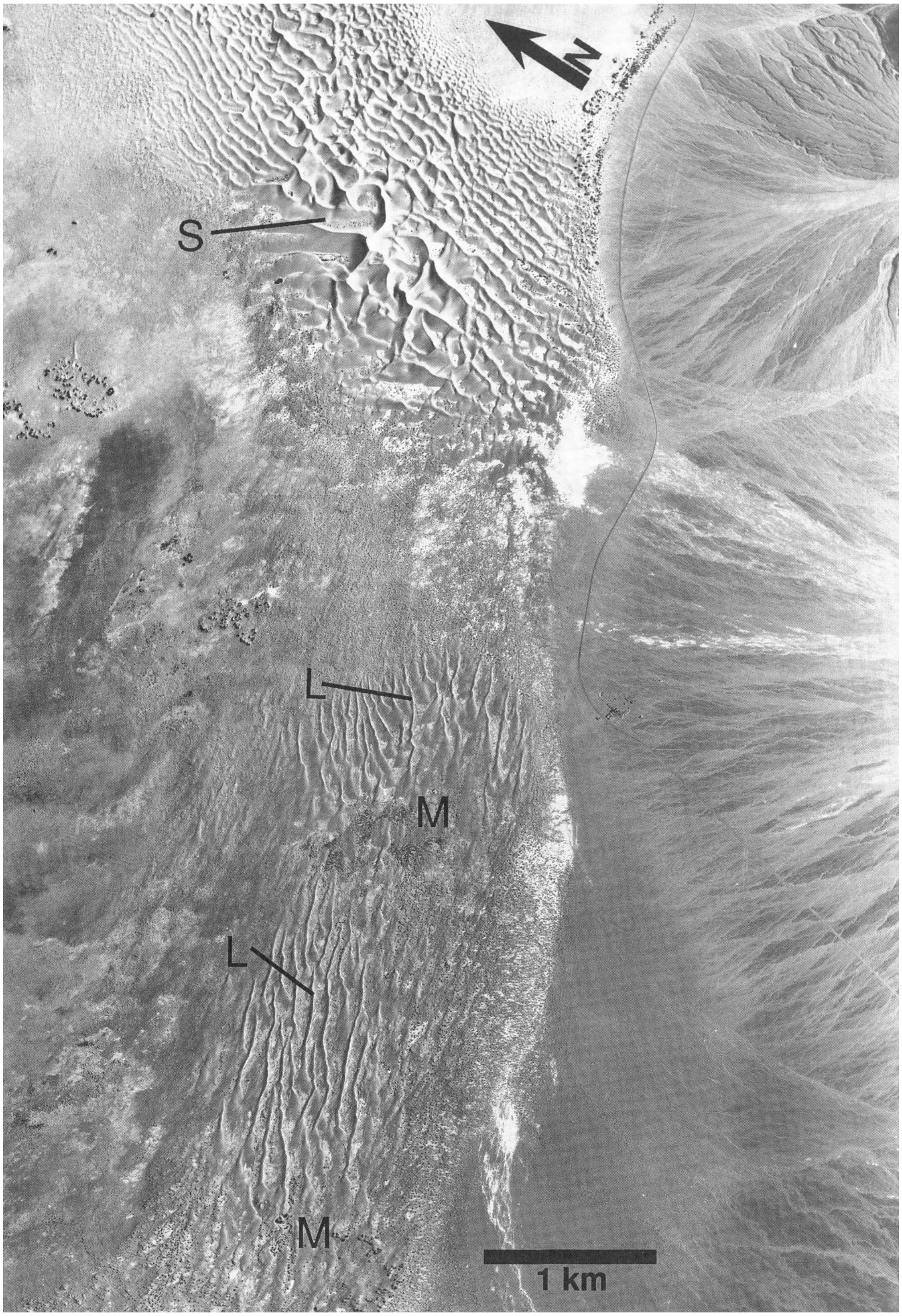

Figure 6. Star (S) and linear (L) dunes of the Stovepipe Wells dune field in northern Death Valley, California (36.7°N, 117.1°W). The dune field also contains reversing transverse and barchan dunes (not shown; see Blumberg and Greeley 1993). The largest of the star dunes is about 40 m high. The linear dunes appear to be extended from masses (M) of low, modified barchanoid dunes similar to what is seen in Figures 3 and 7. The linear dunes formed under the influence of a bimodal distribution of winds funneled into the valley from the northwest and southwest. The star dunes are influenced by the same winds, but modified by a backflow of wind encountering topographic obstacles (mountains) which surround the northern part of the valley, and/or by easterly winds blowing from the main part of Death Valley. Illumination is from the upper right. Portion of aerial photograph obtained in December 1948, available as frame IF-I-42 from the EROS Data Center, Sioux Falls, South Dakota.

Valley illustrate a complex situation that may be somewhat similar to the martian dunes in Figure 3 because topography has played an important role in creating local wind conditions that are different from the regional winds.

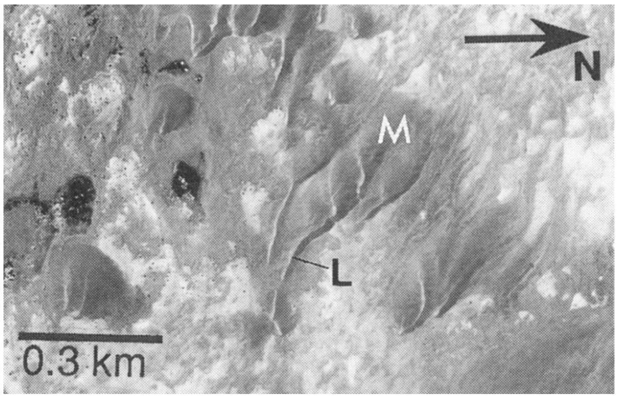

Figure 7. Modified dune mass (M) becoming linear (L) downwind among the Shifting Sand Dunes of Christmas Lake Valley, Oregon. Field examination shows that the linear ridges are seif dunes. These dunes resemble the martian dunes in Figure 3. The highest dune (center) rises nearly 17 m above the surrounding light-toned interdune surfaces. Illumination is from the upper left. Portion of aerial photograph centered at 43.3°N, 120.4°W, obtained on September 21, 1991, by the NASA Ames Research Center Earth Resources Aircraft C-130B Program, Flight 91-010-16, Accession 4347, Sensor 75, Zeiss frame 693.

In Figure 3, we have identified three gaps in the wall of the crater that contains the linear dunes. One of these gaps occurs in the southeastern rim of the crater; the other two are on the southwestern side. The two southernmost gaps, one on the southeast and the other on the southwest rim, are located such that winds can come through them and act directly on the linear dunes and large dune mass from which the linear dunes originate ("M" in Figure 3a). However, these two southern gaps are minor in terms of apparent depth-to-width relative to the third gap, and thus their effect on the large dune mass ("M" in Figure 3a) might not be as important to the overall history of the dune field. The third gap has probably had a more important influence, particularly in creating the transverse dunes ("T_1" and "T_2" in Figure 3) downwind of the linear dunes (L). The third gap, occurring north of the southwestern gap on the west–southwest side of the crater rim, appears to be deeper (or more channel-like) than the other two (Figure 3b) and has not counterpart on the east side of the crater. Winds channelized through this third gap, particularly during southern autumn, would add an extra southwesterly component to the northern end of the dune field. Because there is no similar gap on the east side of the crater, there is probably no significant (i.e., strong) southeasterly contributor to the transverse dunes. Southwesterly winds channelized through the third gap in the southwestern crater rim may have been responsible for the downwind modification of linear dunes into transverse dunes and contributed to the formation of the second transverse dune field ("T_2" in Figure 3a).

The linear dunes in Figure 3 appear to emanate from a dune mass (M) that once may have had the morphology of a transverse dune field similar to those seen in other Hellespontus dune fields to the north (see Edgett and Christensen 1991, Fig. 4). The analogy with dunes in Christmas Lake Valley, Oregon (Figure 7), also suggests that the dune field in Figure 3 once had a transverse morphology. It is likewise curious that the dune mass (M) is located on the southern side of the crater floor, yet the regional winds are from the south. For the dune mass to occur on the southern side of the crater, it must have once been subject to winds from the north. It appears that this dune field might be undergoing a process of redistribution from the south to the north, as evidenced by the formation of the small transverse dune field on the northern side of the crater (T_2). If so, then we speculate that the wind direction in the vicinity of this crater changed relatively recently in martian history. Thomas (1981) suggested that dunes in the southern high latitudes might move from one part of a crater to another on 50,000 to several hundred thousand year time scales. Perhaps Figure 3 is showing an example of a dune field that is actually in the midst of such a redistribution process. Thomas (1981) was describing reorientations that might occur as the dominant southern high latitude wind shifts from southwesterly to southeasterly. However, the dune mass in Figure 3 seems to indicate a different history, one of shifting a dune mass (M) that was originally related to a northerly wind. How long ago in the past this northerly wind might have occurred is unknown.

Our interpretation of present and historical wind flow in the vicinity of the linear dunes observed in Figure 3 is necessarily speculative. It is important to note that, like the star dunes in Figure 2, the linear dunes are a rare occurrence and their morphology is probably influenced by interactions between wind and local topography. Future study of the dunes in Figure 3 will focus on the amount of sand present and the rate at which it is being redistributed from south to north.

Implications

Additional Star and Linear Dunes on Mars?

Two examples presented in this article (Figures 2 and 3) establish the fact that linear dunes and star dunes occur on Mars. The linear dunes identified by Lee and Thomas (1994) are additional examples which demonstrate that such dunes occur on Mars in localized settings. Characterization of the variety of dune forms that exist on Mars is potentially valuable for understanding both current and relatively recent past climate conditions. Specific observations that would be useful to obtain on future Mars-orbiting or -airborne spacecraft include high spatial resolution imaging (better than 20 m/pixel) and stereo imaging or other means (e.g., laser or radar altimetry) to obtain high vertical- and horizontal-resolution (better than 1 m) topographic information. Topographic observations of dunes and their surrounding terrains would be useful. With regard to high-resolution imaging, it is important to note that the image that revealed star dunes (Figure 2) has a resolution of only ~14 m/pixel and that their

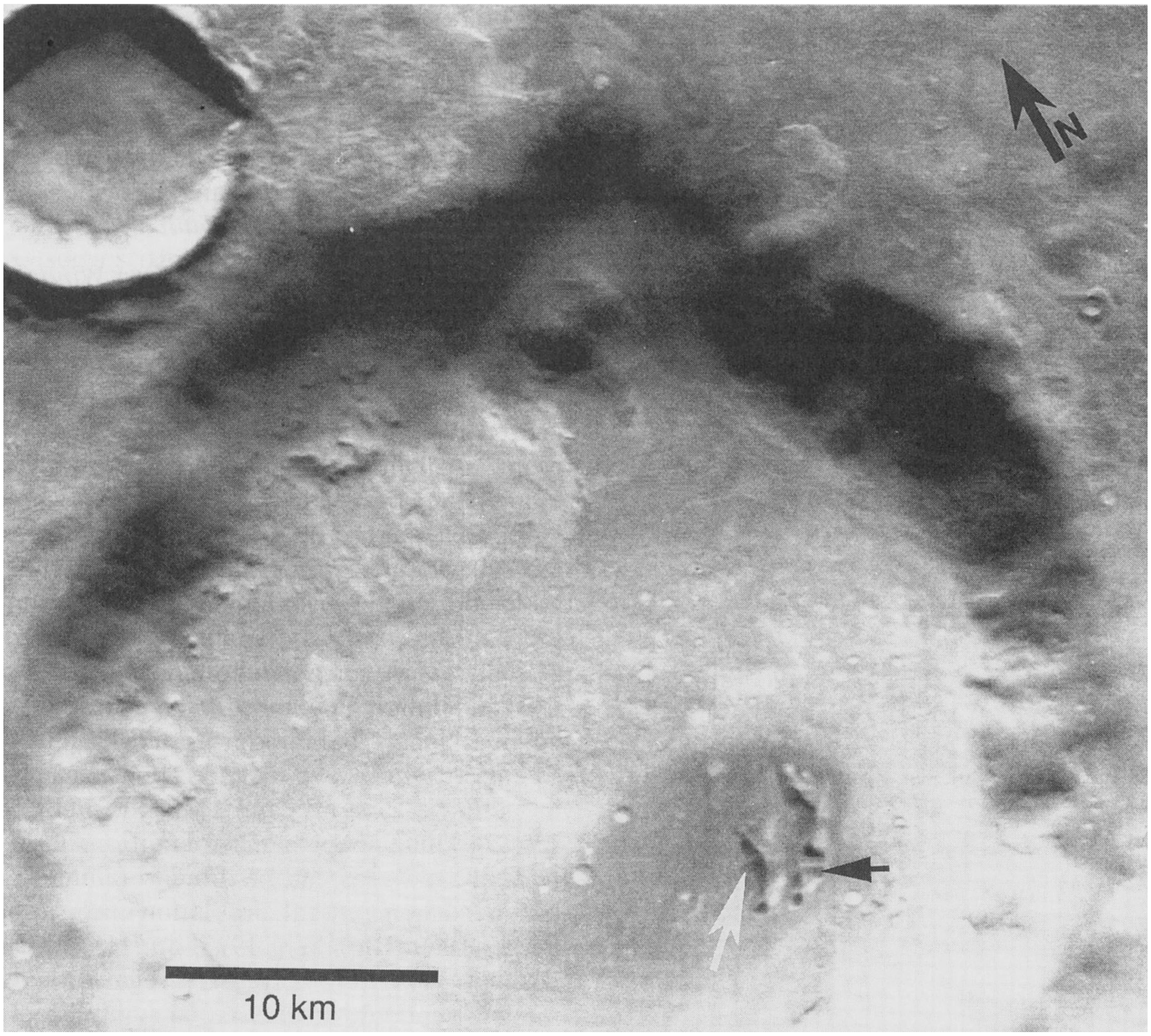

Figure 8. Large barchan with incipient third arm (white arrow) on the floor of a crater at 49.0°S, 340.5°W. Note the square feature which obscures part of the third dune (black arrow); this image artifact is to be ignored. Viking image 575B57; illumination is from the top.

star forms would not have been seen in images with typical Viking orbiter resolutions (90–200 m/pixel).

When making high-resolution observations of a planetary surface, it is important to identify targets that may help meet the study objectives. In addition to the two dune fields described above and the linear dunes of Lee and Thomas (1994), we have identified six martian dune fields which show evidence of polymodal wind action in the form of star and star-like morphologies. These six dune fields should be important targets for future study of dunes on Mars.

The first dune field (Figure 4), located in Darwin Crater at 57.5°S, 19.8°W, was identified by Breed et al. (1982) as a possible star dune. If the dune in Figure 4 is indeed a star dune, it would be of a more complex variety than the star dunes described in Figure 2. A simple star dune is found in a crater south of Kaiser Crater in Hellespontus at 49.0°S, 340.5°W (Figure 8). The largest dune field in Figure 8 is a barchan modified by having a small, incipient third arm protruding from its western side; this dune resembles both the star dunes in Figure 2 and the terrestrial star-like dunes near Bruneau, Idaho (see Greeley et al. 1971, Smith 1982).

A complex dune field that occurs at the southern margin of the Apollinaris Sulci yardang region (12.7°S, 181.8°W) is shown in Figure 9. This dune field should be compared with the aerial photograph of the Dumont, California, dune field described by Nielson and Kocurek (1987, Fig. 1). The pyramidal masses at the center of this dune field (Figure 9) are probably complex star dunes. The dunes northwest of Gordii Dorsum (Figure 10; located at 11.2°N, 147.9°W) are even more complex than those in Figure 9. These dunes have sinuous, intersecting ridges which resemble the dune patterns in the vicinity of the large star dune in the Stovepipe Wells dune field shown in Figure 6.

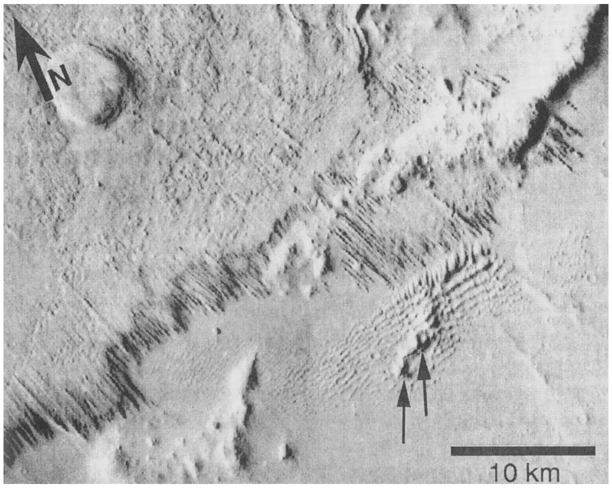

Figure 9. Dune field south of the Apollinaris Sulci near 12.7°S, 181.8°W. The linear features oriented north–south are yardangs. The dune field includes compound star-like features (arrows) resembling the dunes of Dumont, California (see Nielson and Kocurek 1987). Portion of Viking image 436S03; illumination is from the right.

We speculate that star dunes might also occur in the potentially large (up to 25,000 km^2; Peterfreund 1985) sand sea of central Syrtis Major. A single high-resolution image (Figure 11) reveals that the darkest portion of Syrtis Major, a low-albedo strip ~200 km long by 50 km wide oriented northwest–southeast between Nili and Meroe Paterae is a dune field (Peterfreund 1981). The resolution of Figure 11 is insufficient to rule out the possibility that some of the dunes seen there are star dunes rather than transverse dunes. The general circulation modeling described by Skypeck (1989) and Greeley et al. (1993) shows that winds through the Syrtis Major region have some degree of directional variability as a function of season (Nili dunes, Table 1). However, like the region in which the star dunes of Figure 2 occur, the GCM predicts that there is only one dominant wind, and it occurs during northern winter. The probable abundance of sand in Syrtis Major (Lee 1986) and the likely topographic influences of the Nili Patera caldera and adjacent ridge structures make it possible that the local wind regime in central Syrtis Major might be complex enough to create star dunes.

Finally, dunes in the Hellespontus crater Kaiser (46.5°S, 340.5°W), seen in the northern half of Viking image 575B60 (not shown here; see Edgett and Christensen 1991, Fig. 5), have two intersecting orientations with complex ridge forms superposed on them. This particular portion of the Kaiser Crater dune field bears some resemblance to the star dune chains seen in the Gran Desierto of Mexico (Lancaster et al. 1987, Blount 1988, Lancaster 1989b). Perhaps these dunes indicate a local, if not regional, change in wind directionality sometime in the relatively recent martian past.

Martian Sand Supply and Modern Wind Regimes

The presence (and nature of occurrence) of linear and star dune morphologies on Mars adds to our understanding of martian wind regime and sand supply. The shape of a dune is mostly influenced by the aridity of the environment, availability of unconsolidated sand, and directionality of the strongest winds (Fryberger 1979, Wasson and Hyde 1983, Lancaster 1993). Aridity is probably only a factor on Earth, because it is a control on vegetation cover which, in turn, is an important control on dune morphology.

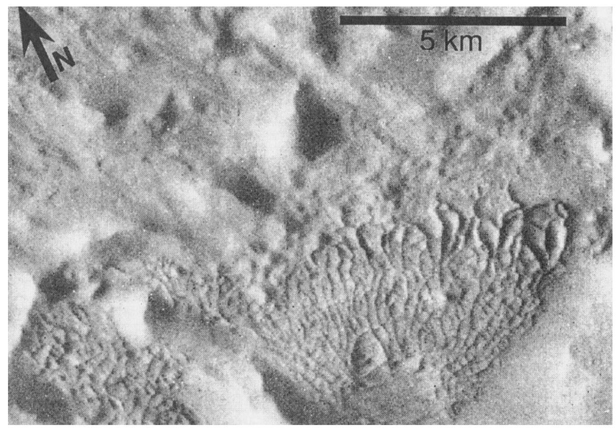

Figure 10. Complex, intersecting dune ridges of possible linear or stellate form. Compare these dunes with the ridges in the vicinity of the star dune in Stovepipe Wells, California, in Figure 6. This is a part of Viking image 693A34, centered near 11.2°N, 147.9°W; illumination is from the right.

"Wind regime" is a general term referring to the velocity distribution and directional variability of wind in a given region or location (Pye and Tsoar 1990, p. 139). The strongest winds, typically associated with storm fronts, move loose sand (Wilson 1971, Pye and Tsoar 1990, p. 15–26). Dune shapes and orientations in most active terrestrial sand seas can be directly related to the influence of the modern general circulation of the atmosphere (Fryberger 1979, Blumberg 1993, p. 111–140, Blumberg and Greeley 1994). For any given region, the winds are unimodal, bimodal, or polymodal (multidirectional). Within a given region, the wind regime may be variable as a function of local topographic influences.

The definition of "sand supply" is somewhat ambiguous. Sand supply is a measure of (1) the volume of sand found in a unit area of the dune field (Wasson and Hyde 1983), (2) the total volume of potentially erodible sand per unit area of dune field, (3) the fraction of a dune field that is covered by erodible sand, (4) the rate at which sand is added to a unit width of dune field from an upwind source, or (5) the rate at which sand accumulates in the dune field (Rubin 1984).

Figure 11. Nili Patera dune field in Syrtis Major (8.9°N, 292.8°W). The resolution of this image is insufficient to make an unambiguous interpretation of dune type based on morphology, but some dunes resemble stars at the very limits of resolution (arrows). The winds in this region change direction according to season (Table 1), and they are probably under the influence of the local topography (Nili caldera). This may be a site to search for star dunes among high-resolution images that might be obtained by future spacecraft missions. Viking image 716A12; illumination is from the left.

Wasson and Hyde (1983) found a significant relationship between the volume of sand per unit area of dune field and the morphology of the dunes present, thus relating dune shape to at least one definition of "sand supply." Barchan dunes are considered to be the result of a limited sand supply. There is a continuum of dune forms from barchan to transverse ridges, indicating successively larger sand supplies in unimodal wind regimes (Wasson and Hyde 1983). Linear dunes generally indicate a limited sand supply in a bidirectional wind regime, while star dunes form where sand is abundant and wind direction is variable (Wasson and Hyde 1983). Barchans may be thought of as "sand-moving" dunes, linear dunes as "passing sand" along their lengths, and star dunes as concentrators of sand (Thomas 1989). It is possible that sand supply among barchans only appears to be lower than among star dunes because barchans are transporting a volume of sand across a surface, while star dunes are sites of sand accumulation with little lateral transport (Thomas 1989).

The linear and star dune morphologies described here (Figures 2 and 3) suggest that both regional wind regimes and topographic influences on local wind regimes are important contributors to the observed dune morphologies. The settings in which the star and linear dune examples illustrated in Figures 2 and 3 occur do not resemble those of the large sand seas in Asia, Africa, and Australia (e.g., Breed et al. 1979a, 1979b, Wasson et al. 1988, Lancaster 1989c). Instead, these settings are similar to those that contain the large dune forms and small sand seas found in North American deserts (Smith 1982). The desert dunes in North America, such as those at Kelso, California (Sharp 1966, Lancaster 1993), Dumont, California (Nielson and Kocurek 1987), Bruneau, Idaho (Greeley et al. 1971, Murphy and Greeley 1972, Murphy 1975), and the Christmas Lake Valley (Figure 7) and Stovepipe Wells (Figure 6) dunes discussed above, are smaller and contain much less sand than the dune fields in the larger terrestrial sand seas. These North American examples thus have had a more limited sand supply. The same is probably also try of dunes on Mars, as suggested by Peterfreund et al. (1981).

Wind regime is related to the general circulation of the martian atmosphere, which has a direct effect on the erosion, transportation, and deposition of aeolian sediments. This circulation affects the distribution of wind streaks and the bright and dark albedo patterns on the martian surface (e.g., Greeley et al. 1992, Kahn et al. 1992). General circulation models such as the Pollack et al. (1990) Mars GCM can be evaluated in terms of whether its results are corroborated by wind-related features seen on the martian surface. Note that the magnitudes of surface shear stress predicted by the GCM are not great enough to move sand on Mars (Skypeck 1989). The minimum shear stress needed to move sand ~160 µm in size is about 550×10^{-4} N m^{-2} (Skypeck 1989, Greeley et al. 1993), while the maximum modeled shear stress in the vicinity of the linear dunes at 59.4°S, 343°W is only 105×10^{-4} N m^{-2} (Figure 4). The GCM results shown by Greeley et al. (1993) are given in bins of 7° latitude by 9° longitude and averaged over a period of several days; thus we should not expect that the GCM will predict sand movement if the winds required to move sand occur at smaller spatial or temporal scales. Instead, we use the GCM to gain insight into the directionality and relative magnitude of regional winds which might affect dunes observed on the martian surface. The primary value of the Mars GCM, therefore, may be in its ability to illuminate rather than predict or be validated by our understanding of Mars surface–atmosphere interactions (see Oreskes et al. 1994).

Skypeck (1989) and Greeley et al. (1993) compared GCM results for direction and relative magnitude of surface shear stress as a function of location and season with (1) the distribution and temporal variations in bright and dark wind streaks, (2) yardangs, and (3) the rock abundances modeled by Christensen (1986). One comparison they did not make, however, is with the low-albedo, sandy deposits which occur on crater floors (Thomas 1984, Edgett and Christensen 1994).

In the middle and equatorial latitudes of Mars (±60°), the GCM results presented by Greeley et al. (1993) corroborate the hypothesis that the strongest winds occur in southern summer, the same season in which major dust storms occur (Kahn et al. 1992). The direction of wind movement during southern summer (see Greeley et al. 1993, Fig. 2e) corresponds to the orientations of dark intracrater deposits commonly referred to as "splotches" (Arvidson 1974, Thomas 1982).

The observation that sandy deposits on crater floors are aligned with the same strong, modern southern summer winds responsible for major dust storms suggests that sand movement is currently (or was recently) an active process on Mars. Whether aeolian sand movement occurs under present martian conditions was further discussed above and in recent articles by Edgett and Christensen (1994) and Lee and Thomas (1994). Major desert regions on Earth, such as the Sahara in northern Africa, also exhibit sand flow and deposition patterns that are directed by the strongest seasonal winds (e.g., Wilson 1971, Mainguet 1978, 1984).

The major terrestrial sand seas that contain linear and star dunes occur where there are strong multidirectional winds, usually resulting from shifts in the strongest wind direction as a function of season (Fryberger 1979). The fact that there are no major sand seas containing linear or star dunes on Mars is an indicator (independent of the GCM) that the dominant martian winds are unidirectional. The star dune field described here (Figure 2) occurs in a regionally unidirectional wind regime (Figure 5), but star dunes were apparently created in a local wind regime influenced by topography. The linear dune field described here (Figure 3) occurs in a region where the GCM suggests the presence of a bimodal wind regime, with the more dominant winds occurring during southern autumn and winter (Figure 5). Perhaps we do not see other linear dune fields in this region or at this latitude (60°S) because there are few large dune fields present or imaged at sufficient resolution to detect them.

Summary

(1) Although rare, star and linear dunes occur on Mars. They are found only in local settings, similar to the occurrence of star and linear dunes in the North American Basin and Range on Earth. There are no major sand seas composed almost entirely of linear or star dunes, as are found on Earth in Australia, Africa, and Asia.

(2) Viking images of Mars reveal at least seven (and perhaps nine or more) occurrences of star and linear dune fields. In this article, we focused on one well-defined example of each. Another occurrence of linear dunes was discussed by Lee and Thomas (1994), and additional localized occurrences of star or star-like dunes were identified and briefly described in this article (including one previously mentioned by Breed et al. 1982).

(3) A field of 11 dunes is located in a valley at 8.8°S, 270.9°W. The dunes begin at the upwind (west) end of the valley as barchans. The barchans grade downwind (southeastward) into incipient stars, which further downwind grade into three-armed star dunes. The progression from barchans to stars corresponds to increasing topographic confinement of the dune sand. The local topography probably acts to create a locally polymodal wind regime in an otherwise unimodal (regional) wind regime. Thus these dunes illustrate and corroborate the model of Lancaster (1989a) that star dunes form by movement of transverse dune forms into complex wind regimes.

(4) The star dunes in the valley at 8.8°S, 270.9°W are probably active, as suggested by the occurrence of dark streaks emanating from the dunes. These dark streaks almost certainly postdate the global dust storms of 1977, and were observed by Viking 1 in 1978. The dark streaks indicate that a minor (unquantifiable) amount of sand was blown from the star dunes and eroded or disrupted the high-albedo materials found on the downwind non-dune surfaces.

(5) The most unambiguous examples of linear seif dunes on Mars occur in a crater located at 59.4°S, 343°W. The linear dunes have formed by modification of a formerly transverse dune mass. The linear dunes indicate a bimodal wind regime, and this is corroborated by the Pollack et al. (1990) general circulation model results as presented by Skypeck (1989) and Greeley et al. (1993). A field of transverse dunes occurring downwind of the linear dunes may have formed under the influence of southwesterly winds channelized through a gap in the nearby crater wall.

(6) The dune mass at 59.4°S, 343°W (from which the linear dunes are being extended) is located at the southern end of the crater floor. The linear dunes and transverse dunes downwind of this mass occur to the north. Most intracrater dune fields on Mars are considered to occur on the downwind side of crater floors (Arvidson 1974, Thomas 1984, Edgett and Christensen 1994). The dune mass ("M" in Figure 3) defies this trend. We speculate that this dune mass formed under conditions when the dominant winds came from a northerly direction. The present southerly winds are causing the formation of linear and transverse dunes downwind (to the north) by erosion and redistribution of sand from the large dune mass. The implication of this speculation is that the regional wind direction has shifted from northerly to southerly sometime in the relatively recent past. A subject of future work will be to explore the question of how long ago this shift might have occurred.

Acknowledgments. We appreciated thoughtful reviews by P. Thomas and N. Lancaster. D. Ball assisted with photograph preparation. We thank P. R. Christensen and R. Greeley for their encouragement and support through the NASA Planetary Geology and Geophysics Program.

References

Allison, I. S. (1966) *Fossil Lake, Oregon: It's Geology and Fossil Faunas*, Oregon State University Press, Corvallis.

Antoniadi, E. M. (1930) *La Planète Mars*, Hermann, Paris.

Arvidson, R. E. (1974) Wind-blown streaks, splotches, and associated craters on Mars: Statistical analysis of Mariner 9 photographs, *Icarus 21*, 17–27, doi:10.1016/0019-1035(74)90086-4.

Bagnold, R. A. (1941) *The Physics of Blown Sand and Desert Dunes*, Methuen, London.

Berry, D. W. (1963) *An Ecological Study of a Disjunct Ponderosa Pine Forest in the Northern Great Basin*, Ph.D. dissertation, Oregon State University, Corvallis.

Blount, H. G. II (1988) *Regional Aeolian Dynamics from Remote Sensing: Origin of the Gran Desierto, Mexico*, Ph.D. dissertation, Arizona State University, Tempe.

Blumberg, D. G. (1993) *Predications of Aeolian Processes by Remote Sensing and Models*, Ph.D. dissertation, Arizona State University, Tempe.

Blumberg, D. G. and R. Greeley (1993) AIRSAR views of aeolian terrain, in *Summaries of the Fourth Annual JPL Airborne Geoscience Workshop, Volume 3: AIRSAR Workshop*, edited by J. van Zyl, *Jet Propulsion Laboratory Publication 93-26*, 9–12, California Institute of Technology Jet Propulsion Laboratory, Pasadena, California.

Blumberg, D. G. and R. Greeley (1994) A comparison of general circulation model predictions to sand drift and dune orientations, *Journal of Climate*, in press. (Later published in:1996, *Journal of Climate 9*(12), 3248—3259, doi: 10.1175/1520-0442(1996)009<3248:ACOGCM>2.0.CO;2.

Breed, C. S. (1977) Terrestrial analogs of the Hellespontus dunes, Mars, *Icarus 30*, 326–340, doi:10.1016/0019-1035(77)90168-3.

Breed, C. S., S. G. Fryberger, S. Andrews, C. McCauley, F. Lennartz, D. Gebel and K. Horstman (1979a) Regional studies of sand seas using Landsat (ERTS) imagery, in *A Study of Global Sand Seas*, edited by E. D. McKee, *United States Geological Survey Paper 1052*, 305–397.

Breed, C. S., M. J. Grolier, and J. F. McCauley (1979b) Morphology and distribution of common 'sand' dunes on Mars: Comparison with the Earth, *Journal of Geophysical Research 84*(B14), 8183–8204, doi:10.1029/JB084iB14p08183.

Breed, C. S. and T. Grow (1979) Morphology and distribution of dunes in sand seas observed by remote sensing, in *A Study of Global Sand Seas*, edited by E. D. McKee, *United States Geological Survey Paper 1052*, 253–302.

Breed, C. S., J. F. McCauley, and M. J. Grolier (1982) Relict drainages, conical hills, and the eolian veneer in Southwest Egypt—Applications to Mars, *Journal of Geophysical Research 87*(B12), 9929–9950, doi:10.1029/JB087iB12p09929.

Christensen, P. R. (1986) The spatial distribution of rocks on Mars, *Icarus 68*, 217–238, doi:10.1016/0019-1035(86)90020-5.

Cutts, J. A. and R. S. U. Smith (1973) Eolian deposits and dunes on Mars, *Journal of Geophysical Research 78*(20), 4139–4154, doi:10.1029/JB078i020p04139.

Edgett, K. S. and P. R. Christensen (1991) The particle size of martian aeolian dunes, *Journal of Geophysical Research 96*(E5), 22,765–22,776, doi:10.1029/91JE02412.

Edgett, K. S. and P. R. Christensen (1994) Mars aeolian sand: Regional variations among dark-hued crater floor features, *Journal of Geophysical Research 99*(E1), 1997–2018, doi:10.1029/93JE03094.

Forbes, C. F. (1973) *Pleistocene Shoreline Morphology of the Fort Rock Basin, Oregon*, Ph.D. dissertation, University of Oregon, Eugene.

Fryberger, S. G. (1979) Dune forms and wind regime, in *A Study of Global Sand Seas*, edited by E. D. McKee, *United States Geological Survey Paper 1052*, 137–169.

Greeley, R., J. D. Iversen, J. B. Pollack, N. Udovich, and B. White (1974) Wind tunnel studies of martian aeolian processes, *Proceedings of the Royal Society, London, Series A* 341, 331–360, doi:10.1098/rspa.1974.0191.

Greeley, R., D. E. Koscielniak, and D. S. Hodge (1971) Bruneau sand dune field, Idaho, and its possible implications in martian geology, *Eos, Transactions of the American Geophysical Union* 52, 860.

Greeley, R., N. Lancaster, S. Lee, and P. Thomas (1992) Martian aeolian processes, sediments, and features, in *Mars*, edited by H. H. Kieffer, B. M. Jakosky, C. W. Snyder, and M. S. Matthews, p. 730–766, University of Arizona Press, Tucson.

Greeley, R., A. Skypeck, and J. B. Pollack (1993) Martian aeolian features and deposits: Comparisons with general circulation model results, *Journal of Geophysical Research 98*(E2), 3183–3196, doi:10.1029/92JE02580.

Kahn, R. A., T. Z. Martin, R. W. Zurek, and S. W. Lee (1992) The martian dust cycle, in *Mars*, edited by H. H. Kieffer, B. M. Jakosky, C. W. Snyder, and M. S. Matthews, p. 1017–1053, University of Arizona Press, Tucson.

Kargel, J. S. and R. G. Strom (1992) Ancient glaciation on Mars, *Geology 20*(1), 3–7, doi:10.1130/0091-7613(1992)020<0003:AGOM>2.3.CO;2.

Lancaster, N. (1982) Linear dunes, *Progress in Physical Geography 6*(4), 476–504, doi:10.1177/030913338200600401.

Lancaster, N. (1989a) Star dunes, *Progress in Physical Geography 13*(1), 67–91, doi:10.1177/030913338901300105.

Lancaster, N. (1989b) The dynamics of star dunes: An example from the Gran Desierto, Mexico, *Sedimentology 36*(2), 273–289, doi:10.1111/j.1365-3091.1989.tb00607.x.

Lancaster, N. (1989c) *The Namib Sand Sea*, A. A. Balkema, Rotterdam.

Lancaster, N. (1993) Kelso dunes, *National Geographic Research and Exploration 9*, 444–459.

Lancaster, N. and R. Greeley (1987) Mars: Morphology of southern hemisphere intracrater dune fields, *Reports of Planetary Geology and Geophysics Program—1986*, in *NASA Technical Memorandum 89810*, 264–265.

Lancaster, N., R. Greeley, and P. R. Christensen (1987) Dunes of the Gran Desierto Sand Sea, Sonora, Mexico, *Earth Surface Processes and Landforms 12*(3), 277–288, doi:10.1002/esp.3290120306.

Lee, P. and P. C. Thomas (1994) Longitudinal dunes on Mars and the current geological effectiveness of martian winds, submitted for publication. (Later published in: 1995, *Journal of Geophysical Research 100*(E3), 5381–5395, doi:10.1029/95JE00225)

Lee, P., P. C. Thomas, J. Veverka, and S. Calvo (1993) Discovery of longitudinal dunes on Mars, abstract 04.02, *Bulletin of the American Astronomical Society 25*, 1038.

Lee, S. W. (1986) IRTM observations of Syrtis Major: An active aeolian environment, *Reports of Planetary Geology and Geophysics Program—1985*, in *NASA Technical Memorandum 88383*, 532–534.

Mainguet, M. (1978) The influence of trade winds, local air masses and topographic obstacles on the aeolian movement of sand particles and the origin and distribution of dunes and ergs in the Sahara and Australia, *Geoforum 9*(1), 17–28, doi:10.1016/0016-7185(78)90021-0.

Mainguet, M. (1984) Space observation of Saharan aeolian dynamics, in *Desert and Arid Lands*, edited by F. El-Baz, p. 59–77, Nijhoff, The Hague.

McKee, E. D. (1979) Introduction to a study of global sand seas, in *A Study of Global Sand Seas*, edited by E. D. McKee, *U. S. Geological Survey Professional Paper 1052*, 1–19.

Murphy, J. D. (1975) The geology of Bruneau Dunes State Natural Park, Idaho, *Geological Society of America Abstracts with Programs 7*, 633.

Murphy, J. D. and R. Greeley (1972) Sand dunes at Eagle Cove (Bruneau), Idaho: Possible analogs to martian eolian features, *Eos, Transactions of the American Geophysical Union 53*, 1035.

Nielson, J. and G. Kocurek (1987) Surface processes, deposits, and development of star dunes: Dumont dune field, California, *Geological Society of America Bulletin 99*(2), 177–186, doi:10.1130/0016-7606(1987)99<177:SPDADO>2.0.CO;2.

Oreskes, N., K. Shrader–Frechette, and K. Belitz (1994) Verification, validation, and confirmation of numerical models in the earth sciences, *Science 263*, 641–646, doi:10.1126/science.263.5147.641.

Peterfreund, A. R. (1981) Visual and infrared observations of wind streaks on Mars, *Icarus 45*, 447–467, doi:10.1016/0019-1035(81)90046-4.

Peterfreund, A. R. (1985) *Contemporary Aeolian Processes on Mars: Local Dust Storms*, Ph.D. dissertation, Arizona State University, Tempe.

Peterfreund, A. R., R. Greeley, and D. Krinsley (1981) Martian sediments: Evidence for sand on Mars, *Reports of Planetary*

Geology Program—1981, in *NASA Technical Memorandum 84211*, 205–207.

Pollack, J. B., R. M. Haberle, J. Schaeffer, and H. Lee (1990) Simulation of the general circulation of the martian atmosphere, 1, polar processes, *Journal of Geophysical Research 95*(B2), 1447–1473, doi:10.1029/JB095iB02p01447.

Pye, K. and H. Tsoar (1990) *Aeolian Sand and Sand Dunes*, Unwin and Hyman, London.

Rice, J. W., Jr., and J. D. Mollard (1994) Analogs and interpretations for the martian thumbprint terrain and sinuous ridges, *Lunar and Planetary Science 25*, 1127–1128, Lunar and Planetary Institute, Houston, Texas.

Rubin, D. (1984) Factors determining desert dune type, *Nature 309*, 91–92, doi:10.1038/309091a0.

Ruff, S. W. (1992) Dorsa Argentea type sinuous ridges, Mars: Evidence for linear dune hypothesis, in *Workshop on the Martian Surface and Atmosphere Through Time*, edited by R. M. Haberle and B. M. Jakosky, *Lunar and Planetary Institute Technical Report 92-02*, 126–127, Houston, Texas.

Ruff, S. W. (1994) Comparison of Mars sinuous ridges with terrestrial linear dunes: Observations from the field, *Lunar and Planetary Science 25*, 1171–1172, Lunar and Planetary Institute, Houston, Texas.

Ruff, S. W. and R. Greeley (1990) Sinuous ridges of the south polar region, Mars: Possible origins, *Lunar and Planetary Science 21*, 1047–1048, Lunar and Planetary Institute, Houston, Texas.

Sharp, R. P. (1966) Kelso dunes, Mojave Desert, California, *Geological Society of America Bulletin 77*(10), 1045–1074, doi:10.1130/0016-7606(1966)77[1045:KDMDC]2.0.CO;2.

Skypeck, A. P. (1989) *Comparison of a Mars General Circulation Model with Aeolian Features and Deposits*, M.S. thesis, Arizona State University, Tempe.

Smith, R. S. U. (1982) Sand dunes in the North American deserts, in *Reference Handbook on Deserts of North America*, edited by G. L. Bender, p. 481–524, Greenwood Press, Westport, Connecticut.

Thomas, D. S. G. (1989) Aeolian sand deposits, in *Arid Zone Geomorphology*, edited by D. S. G. Thomas, p. 232–261, Belhaven Press, London.

Thomas, P. (1981) North–south asymmetry of eolian features in martian polar regions: Analysis based on crater-related wind markers, *Icarus 48*, 76–90, doi:10.1016/0019-1035(81)90155-X.

Thomas, P. (1982) Present wind activity on Mars: Relation to large latitudinally zoned sediment deposits, *Journal of Geophysical Research 87*(B12), 9999–10,008, doi:10.1029/JB087iB12p09999.

Thomas, P. (1984) Martian intracrater splotches: Occurrence, morphology, and colors, *Icarus 57*, 205–227, doi:10.1016/0019-1035(84)90066-6.

Tsoar, H. (1983) Dynamic processes acting on a longitudinal (seif) sand dune, *Sedimentology 30*(4), 567–578, 10.1111/j.1365-3091.1983.tb00694.x.

Tsoar, H. (1989) Linear dunes—Forms and formation, *Progress in Physical Geography 13*(4), 507–528, doi:10.1177/030913338901300402.

Tsoar, H. and D. G. Blumberg (1992) Cliff effects on windward transport and accumulation of sand, abstract presented to the *Association of American Geographers 88th Annual Meeting*, San Diego, California, p. 240.

Tsoar, H., R. Greeley, and A. R. Peterfreund (1979) Mars: The north polar sand sea and related wind patterns, *Journal of Geophysical Research 84*(B14), 8167–8180, doi:10.1029/JB084iB14p08167.

Wasson, R. J., K. Fitchett, B. Mackey, and R. Hyde (1988) Large-scale patterns of dune type, spacing, and orientation in the Australian continental dune field, *Australian Geographer 19*(1), 89–104, doi:10.1080/00049188808702952.

Wasson, R. J. and R. Hyde (1983) Factors determining desert dune type, *Nature 304*, 337–339, doi:10.1038/304337a0.

Wilson, I. G. (1971) Desert sandflow basins and a model for the development of ergs, *Geographical Journal 137*, 180–199.

Differences between the © 1994 Academic Press version of the paper and this one:

- the layout/formatting of the document
- Minor changes to the wording of Figure captions were made.
- the reference citations are herein unabbreviated and include digital object identifiers (DOI) for documents for which a DOI was available as of 18 October 2009.